

Load Flow Analysis of Rural Islanded Hybrid Microgrid

Clinton Kum Ngum

Department of Electrical and Electronic Engineering,
Faculty of Engineering and Technology,
University of Buea, Cameroon

Tamanjong Fru Fofang, Suh Elvice Fru

Department of Renewable Energy,
College of Technology,
University of Buea, Cameroon

Abstract: Extension of the utility grid to rural villages is not a viable option due to the high cost involved, coupled with low population density and low electrical energy demand. Isolated power systems such as rural hybrid microgrids based on renewables could be a potential solution. Several factors influence the development of these rural hybrid microgrids such as technical and economic issues. Motivated by these facts, the target of this study is to propose an operational load flow algorithm for rural hybrid microgrids by developing a steady state analysis tool for rural islanded hybrid microgrid systems. To achieve this, the root causes of hybrid system design failures were first investigated and identified through field and literature survey. A generalized load flow algorithm was then developed to monitor the steady state performance of the small rural hybrid power systems. Conventional load flow tools found in literature are generally not suitable for the rural islanded hybrid microgrid operating mode. The reason is that none of these tools reflect the rural islanded hybrid microgrid special philosophy of operation. The proposed load flow algorithm adopts the actual characteristics of the rural islanded hybrid microgrid operation where distributed generation units are controlled using droop control methods and, their generated active and reactive powers are dependent on the power flow variables and cannot be pre-specified. Also, the steady-state system frequency is not constant and is considered as one of the power flow variables. The proposed load flow algorithm is generic, where features of the distribution system such as feeder models and load models have been taken into consideration. Simulation studies show that with drooping coefficients, m_p and n_q at 3% and 2% respectively, the system bus voltages are optimized with a maximum at bus 5 with a p.u voltage of 0.963015 and minimum at bus 3 with p.u voltage of 0.92361 which are comparatively higher than other variations of the drooping coefficients. Also simulation proved that, with a slight increase in the line parameters, there was a further increased in the buses voltage drops. The proposed hybrid system design framework and load flow algorithm can facilitate the successful implementation of hybrid systems for rural electrification

Keywords: Hybrid microgrids, Distributed generation, Generalized load flow algorithm

1. INTRODUCTION

Electricity is the backbone and acute condition for a country's development in terms of economy and good quality of lifestyle for the citizens. The more energy per capita a country consumes, the more developed it is [1]. Access to energy gives access to better standards of living such as access to health, to human security, to information, to wealth and the fuelling of human development in general [2].

According to the World Energy Outlook 2024 [3], 47 countries in Africa do not have full access to electricity. Most are in the Sub-Saharan Africa and mainly in rural or remote areas. Most of them are living in countries of Sub-Saharan Africa and mainly in rural or remote areas. Electrification in remote areas is constrained by technical barriers like long-distant transmission network, rugged terrains, and highly dispersed population. The low population density characterized by a low level of education implies low load density and low revenues. These characteristics hinder investors from investing in the rural sector in Sub-Saharan Africa.

2. LOAD FLOW ANALYSIS IN DISTRIBUTED GENERATION NETWORK

Load Flow in Distributed Generation Network:

Distributed generation refers to electric power generation supplying loads in their neighbourhood [4]. This is the use of small-scale generation systems to produce electricity close to customers. In distributed generation, size and location are not the only novelty as the small-scale generation systems are not centrally dispatched [4]. In the conventional system, the load flow problem involves the computation of voltage magnitudes and phase angles at each bus in a power system under balanced steady-state operation [5]. Once

these quantities are evaluated, the active and reactive power flows through the system elements, such as transmission lines can be deduced. The outcome of this analysis is generally used for the evaluation of steady-state, as well as dynamic performance, of interconnected electric systems [5].

Operating microgrids in islanded mode presents many technical challenges. The core of these technical challenges includes having to regulate the voltage and frequency within standard operating ranges, providing the real and reactive power requirements of the loads within the island and ensuring the availability of an adequate reserve margin within the microgrid [4]. This reserve margin is typically a function of the load factor, the magnitude of the load, the load variation over time, the reliability requirements of the load, and the availability of the distributed generators [4]. The Load flow analyses are performed to investigate these different technical aspects. Conventional algorithms lack the ability to mimic the operating philosophy of islanded microgrids hence specialized methods are employed in load flow modelling of microgrids [4].

The work in [6] elaborates on the various steps to carry out power flow analysis in small and medium size power systems using the Newton-Raphson method of load flow analysis. They concluded that the Newton-Raphson method of power flow analysis was faster on the speed of convergence, but programming is more complex [4] [5]. The application of this system to a small distribution generation network has a major setback since the effects of changes in the system frequency and voltage profile cannot be monitored. The work in [7] focused on the design of a microgrid which consists of wind turbine, PV, micro turbine and proton-exchange membrane (PEM) fuel cell, main grid and load busses.

As shown in Figure 1 [7], the energy sources are connected to the network via an interface unit such as a power electronic device. Power electronic systems affect the quality of the system to which they are connected and require new control arrangements [7], [8]. They used MATLAB and PowerWorld simulator for the load flow study. Since the system is grid tied, the grid provides infinite bus characteristics to the system, hence stabilizing the bus voltages and system frequency. In the absence of the grid, the Microgrid Central Controller (MGCC) controls the Micro-source Controller (MC) and Load Controller (LC) providing system stability, but this system is costly for a rural community.

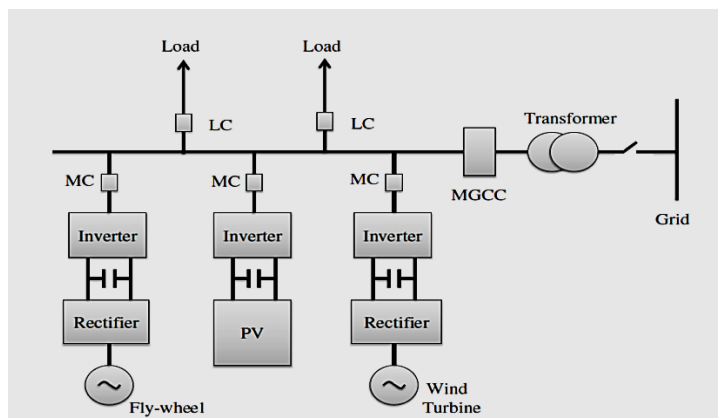


Figure 1: Structure of Typical Microgrid [7]

Including Slack Bus in Distributed Generation network: When a microgrid is connected to the main grid, the frequency and voltage are preserved by the main grid. This means a slack bus is validated as a reference for the system. In a standalone mode, both frequency and voltage are not constant; therefore, conventional power flow methods of analysis cannot be applied [5] [9] [10] [11]. A recent review of the literature on this topic [5] [9] [10] [11] found that power flow regarding islanded microgrid cannot be resolved by conventional power flows such as Newton-Raphson. A fundamental issue of power flow for the islanded microgrid is addressed due to non-constant frequency. If the frequency is not constant, the bus admittance (Y_{bus}) will not be constant since it depends on the frequency [5] [9] [10] [11]. In a microgrid, the busbar classified as slack, PV, or PQ bus in a power flow will be classified as invalid regarding the active and reactive powers, as well as the voltage magnitude and angle of the droop bus. Once these parameters are not possible to be pre-specified, conventional methods are not validated in the case of a standalone microgrid [9].

If assumption is taken that the function of slack bus will be shifted to all PV buses amiable in the system, then it could not be implemented in mathematical modelling of simple Load flow method [11]. This is so because in conventional load flow method, at the starting of iteration for calculating the losses, one bus is kept out of the iteration [5] [11]. All the losses calculated in the iteration are shifted to the slack bus [5] [11]. For slack bus requirement in microgrid, the method of load flow needs to be modified include all buses in the iteration and losses calculated will be shifted to all the possible buses [11].

Distributed Generation network with Storage: Fluctuations and variations in energy generated can be mitigated when associated with energy storage devices [12]. Renewable generation and energy storage devices can behave as a constant power generation plant when working together, depending on the storage system capacity [12] [13]. Energy storage is essential for generation stabilization, power quality assurance, voltage and frequency regulation, load levelling, peak shaving and distribution support [14]. Different energy storage technologies serve applications depending on the amount of energy to be stored, the rate at which this energy will be transferred and the response time [15].

Another purpose of load flow is to balance active and reactive power demand and generation as given by the equations [5].

$$\sum P_G = \sum P_D + P_L \quad (2)$$

$$\sum Q_G = \sum Q_D + Q_L \quad (3)$$

where P_G , Q_G , P_D , Q_D , P_L , Q_L represent active power generated, reactive power generated, active power demand, reactive power demand, active power loss in the system and reactive power loss in the system, respectively.

Droop Control Implementation in Distributed Generation network: Hybrid microgrids need continuous monitoring of their components and surroundings to guarantee efficient energy management [4]. Dedicated sensor network and communication infrastructures are necessary to coordinate the control actions and to broadcast the collected data to the interested partners [4]. In small rural hybrid microgrids, the inclusion of these dedicated sensor networks and communication infrastructure will increase the cost of the system making it too expensive for the rural community. An appropriate load flow algorithm can be implemented to act as a communication medium using droop control techniques in small rural hybrid microgrids [16]. Microgrids comprise distributed generation sources, storage facilities, and associated loads, which can be grouped as a variety of customers, i.e., residential buildings, commercial units, and industrial parks [17]. In the operation mode, the active and reactive power flow, voltage profile, and frequency must be controlled to achieve reliable electric service [18].

During on-grid operation, the main grid ensures that the microgrid operates within the acceptable frequency and voltage ranges. The main grid absorbs/injects the excess/deficit active or reactive power from the microgrid, hence ensuring a balance between power demand and supply. When the hybrid system is operated in on-grid mode, the system tracks the frequency and phase of the prevailing grid voltage at the point of common coupling PCC [4]. A microgrid connected to the main grid “sees” the latter as a generator with infinite capacity. However, when operated in off-grid mode, the microgrid loses the reference bus at the point of common coupling (PCC) [4]. Therefore, in off-grid mode the DG units of the microgrid must assume the role of controlling their active and reactive power supply to meet load demand since no slack bus is available anymore [4]. Droop control uses frequency to control active power flow [19].

$$\omega = \omega_0 - m_p P \quad (4)$$

$$V = V_0 - n_p Q \quad (5)$$

Where ω_0 and V_0 are the reference angular speed and voltage respectively. Coefficients m_p and n_q , on the other hand, are the active and reactive power static droop gains. These gains specify the frequency or voltage slopes of the droop characteristic of the DG unit [19]. The typical droop control characteristic diagrams are depicted in Figure 2.

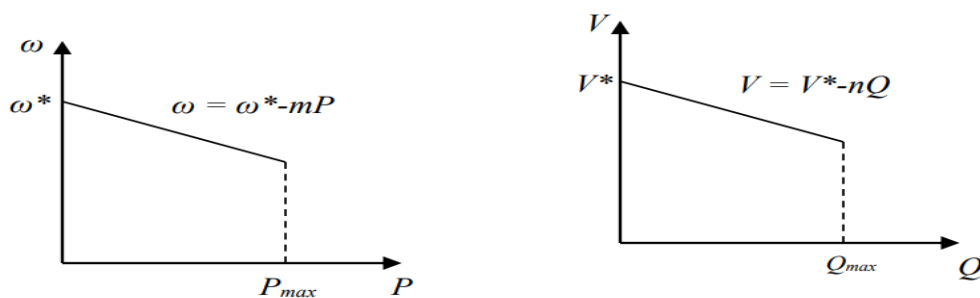


Figure 2: Static Droop Characteristics [19]

Optimal Power Flow Techniques and Limitations

Mehmet et al have presented an Optimal Power Flow (OPF) and load flow analysis of IEEE 30 bus system with DG in which a PV plant is determined as DG plant. According to different PV integration rates, the system parameters were analysed with especially active and reactive losses being investigated. They showed that more than 30% PV contribution in transmission and distribution systems can affect the system adversely and because of this reason, the PV contribution limit is set at 30%. Newton-Raphson (NR) method is used as the load flow analysis method but the emphasis was on generalised DGs and not focussing on DGs for rural electrification. [20].

In another work presented by P. Harish Kumar et al [21] the load flow analysis and distributed generation (DG) allocation in Indian utility 62-bus power system (real distribution system) was performed by using Backwards/Forward Sweep (BFS) methods, NR method and combination of particle swarm optimization algorithm (PSO) with NR method. The solutions obtained using these methods were presented in terms of voltage magnitude, active power, reactive power, phase angle and power losses. The load flow solutions obtained using the above-said methods were validated with the results obtained using continuation power flow (CPF) and evolutionary-based optimal power flow (EOPF) methods, published earlier. From their work, the PSO algorithm was proposed for optimal placement, and sizing of DG with an objective of the power loss reduction and voltage profile improvement. PSO algorithm is used to find out the best location and optimal size of DG. This work although great still falls short of taking into the considerations of rural islanded systems of power distribution.

S. Anbuchandran et al [22] in their work concentrated on optimal placement of DG generators in order to improve system operation. It scratches the surface on presenting the importance of load flow analysis but does not delve into the entireties of the methods of doing so.

In the most recent work carried out by Aya Al Shaltounia et al [23] The optimal power flow for networked microgrids with different renewable energy sources (PV panels and wind turbines), storage systems, generators, and load is investigated in this study. A conventional method and an Artificial Intelligence method are applied to solve the OPF problem. The results showed minimum losses and higher efficiency when performing OPF using Neural Network than the Newton-Raphson method. The efficiency of the power system for the networked MG is 99.3% using Neural Network and 97% using the Newton-Raphson method. The Neural Network method, which mimics how the human brain works based on AI technologies, gave the best results and better efficiency in both cases (Battery as Load/Battery as Source) than the conventional method. However, artificial intelligent methods are still more complex, demanding exceedingly high computational skills and have not fully developed, hence not suitable for small rural islanded hybrid microgrid systems.

Proposed Optimal Load Flow Algorithm for Rural Islanded Hybrid Systems

A new formulation is required to provide a proper load flow analysis in rural islanded hybrid systems taking into consideration their special philosophy of operation. The power produced by the distributed generation units in the islanded hybrid system cannot be pre-specified prior to the solution of the load flow equations. Again, the rural islanded hybrid system has no slack bus capable of maintain a constant system frequency, as such the rural islanded hybrid system steady-state frequency is not pre-specified and is one of the power flow variables. In this section, a novel and generic load flow algorithm is formulated for rural islanded microgrids. The proposed algorithm is novel since it adapts the real characteristics of the rural islanded microgrid operation; i.e., the distributed generation units are controlled using the droop control methods; accordingly their generated active and reactive powers are dependent on the power flow variables and are governed by their droop characteristics; secondly, the system frequency acts as a communication medium between the different DG units in the islanded microgrid and as such the steady-state system frequency is not pre-specified and is considered as one of the power flow variables. The load flow problem is formulated as a set of nonlinear equations describing the power flow problem in the islanded microgrid systems. A convergent Gauss Seidel method is proposed to solve this set of nonlinear equations. The proposed power flow algorithm can be a powerful tool that helps the small rural hybrid network operator to perform the operational analysis for the rural islanded hybrid system with different distributed generation resources operating modes.

3. METHODOLOGY ADOPTED

Rural Islanded Hybrid System Modelling

Feeders modeling: In rural islanded hybrid systems, the system frequency is a power flow variable. Therefore, its variation is taken into account in the line reactance model. The line impedances are converted to admittances.

$$y_{ij} = \frac{1}{Z_{ij}} = \frac{1}{r_{ij} + jx_{ij}} \quad (6)$$

$$Y_{ii} = \sum_{\substack{j=0 \\ j \neq i}}^n y_{ij} \quad (7)$$

For a 3-bus rural power system, the bus admittance matrix can be written as:

$$Y_{bus}(\omega) = \begin{bmatrix} Y_{11} & Y_{12} & Y_{13} \\ Y_{21} & Y_{22} & Y_{23} \\ Y_{31} & Y_{32} & Y_{33} \end{bmatrix} \quad (8)$$

Load modeling: Behavior of loads in a rural hybrid power system can be modeled by representing the changes in their active and reactive power requirements due to changes in system voltages and frequency. The voltage dependency of load characteristics is represented by the static load models expressed as in [24]

$$P_{Li} = P_{oi} |V_i|^{K_{pv}} \quad (9)$$

$$Q_{Li} = Q_{oi} |V_i|^{K_{qv}} \quad (10)$$

Where, P_{oi} and Q_{oi} are the nominal active and reactive power operating points respectively; K_{pv} and K_{qv} are the active and reactive power voltage dependency exponents. In the constant power, constant current and constant impedance models, the active and reactive voltage dependency power exponents are equal to zeros, ones and twos, respectively. The values of the active and reactive power voltage dependency exponents for residential, industrial and commercial loads are given in [24]. The frequency dependency of load characteristics is represented by multiplying the voltage dependent static load model by a factor as follows [24]:

$$P_{Li} = P_{oi} |V_i|^{K_{pv}} (1 + K_{pf} \Delta\omega) \quad (11)$$

$$Q_{Li} = Q_{oi} |V_i|^{K_{qv}} (1 + K_{qf} \Delta\omega) \quad (12)$$

Where $\Delta\omega$ is the angular frequency deviation ($\omega - \omega_0$); K_{pf} ranges from 0 to 3.0, and K_{qf} ranges from -2.0 to 0 [25]. A load class mix of residential, industrial and commercial loads has been adopted in this work to generalize the proposed algorithm and take the impacts of load modeling in consideration. Table 1 shows typically used values for K_{pv} and K_{qv} [25].

Table 1: Typically used values for K_{pv} and K_{qv} [25]

Load Type	K_{pv}	K_{qv}
Constant power	0.00	0.00
Constant Current	1.00	1.00
Residential	0.92	4.04
Commercial	1.51	3.40
Industrial	0.18	6.00

DG modeling: In grid-connected microgrids, given the relatively small sizes of the DG units, they are controlled as PV or PQ buses. On the other hand, in rural islanded hybrid systems, the DG units are operated to achieve appropriate sharing of the load demands and to control the microgrid voltage magnitude and frequency levels. Given that there is no slack bus, it will be impossible to make all DG units operate in PV or PQ modes. Accordingly, in islanded microgrids, the DG units can operate in three modes of operation; i.e., PV, PQ and droop. For DG units operating in PV mode, the DG units inject pre-specified quantity of active power and the required reactive power to bring the bus voltage to a pre-specified voltage value. To take the DG reactive current limits in consideration, the calculated DG reactive power is compared with the minimum and maximum limits. If the calculated reactive

power violates the upper or lower limits, the DG switch from PV to PQ mode and the reactive power is kept at its limits. When the DG operates in PQ mode, the DG unit injects pre-specified quantities of active and reactive powers.

Some of the DG units are interfaced via a power electronic converter and an output filter [26], [27]. A review of possible converter interface arrangements, different control techniques and synchronization algorithms for DG units can be found in [28], [29], [30]. Figure 3 shows the steady-state, fundamental frequency, power flow model of a DG unit operating in droop mode. As shown in the figure 3, the DG units operating in the droop mode, which include the energy resource, the output filter and the power electronic converter, are modeled as an ideal voltage source whose frequency and voltage magnitude are determined using droop. This model is sufficient to compute the steady-state operating point for electrical variables at the PCC of each DG unit operating in droop mode irrespective of the internal power circuit and the control structure used to implement such droop characteristics. For DG units operating in droop mode, the power electronic interface converter, the output filter, the energy resource and the control structure used to implement the droop characteristics at the PCC of the DG unit, do not affect the load flow solution.

In the droop mode of operation, active power sharing is realized by introducing droop characteristics to the frequency of the DG unit output voltage at the PCC such that for the DG unit connected to bus i :

$$\omega = \omega_i^* - m_{pi} P_{Gi} \quad (13)$$

where ω is the DG output voltage frequency, ω_i^* is the no-load nominal frequency set point, m_{pi} is the active power static droop gain, and P_{Gi} is the injected active power by the DG unit. From equation 14, it can be seen that the droop characteristic provide a measure of negative feedback that ensures that all the DG units are producing voltages with the same angular frequency at steady state [8].

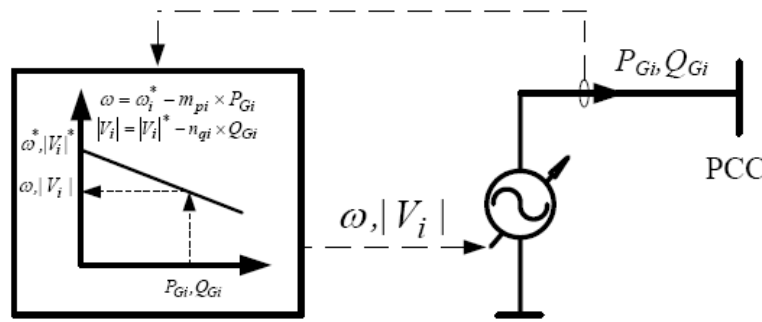


Figure 3: Steady-state, fundamental frequency model of a DG unit operating in droop mode [8]

On the other hand, the reactive power sharing among the different DG units in the hybrid system is achieved through the control of the DG output voltage magnitude. This control is accomplished in a d - q frame that rotates with the angular speed ω . A drooping characteristic is introduced in the voltage magnitude of the DG unit output voltage at the PCC is such that:

$$V_{di} = V_i^* - n_{qi} Q_{Gi}, \quad V_{qi} = 0 \quad (14)$$

where, V_{di} and V_{qi} are the d -axis and q -axis components of the DG output voltage at bus i , respectively, V_i^* stands for the no-load nominal output voltage set point, n_{qi} is the reactive power static droop gain, and Q_{Gi} is the injected reactive power by the DG unit. As per (14), the output voltage magnitude is aligned to the d -axis of the DG reference frame and the output voltage q -axis component is set to zero.

The static droop gains for the DG unit connected to bus i (m_{pi} , n_{qi}) are conventionally calculated based on the allowable voltage and frequency regulation as well as the DG unit capacity [8].

$$m_{pi} = \frac{\omega^{ub} - \omega^{lb}}{P_{Gi,max}}, \quad n_{qi} = \frac{|V_i|^{ub} - |V_i|^{lb}}{Q_{Gi,max}} \quad (15)$$

where ω^{ub} and ω^{lb} are the upper and lower bounds on system frequency, $|V_i|^{ub}$ and $|V_i|^{lb}$ are the upper and lower bounds on allowable voltage magnitudes at bus i , and are the maximum active and reactive power capability of the DG unit. The choice of the minimum and maximum allowable values of the frequency and voltage magnitude depend on the required voltage and frequency regulation [8].

In case of having DG units with different ratings, to achieve proper sharing in proportion to the DG units' ratings, the static droop gains are conventionally chosen as follows:

$$m_{p1}P_{G1,max} = m_{p2}P_{G2,max} = \dots = m_{pi}P_{Gi,max}, \quad \forall i \in B_{droop} \quad (16)$$

$$n_{q1}Q_{G1,max} = n_{q2}Q_{G2,max} = \dots = n_{qi}Q_{Gi,max}, \quad \forall i \in B_{droop} \quad (17)$$

Where B_{droop} is the set of all droop-controlled buses in the system

Based on (17) -(18) the injected active and reactive power from a DG unit i operating with droop control can be expressed in the load flow formulation as follows:

$$P_{Gi} = \frac{1}{m_{pi}}(\omega_i^* - \omega) \quad (18)$$

$$Q_{Gi} = \frac{1}{n_{qi}}(|V_i^*| - |V_i|) \quad (19)$$

Typically, the DG units are equipped with a current limiter to limit the production of the DG unit to its rated active and reactive capacities $P_{Gi,max}$ and $Q_{Gi,max}$. To take the DG current limits in consideration in the power flow formulation, the calculated DG active and reactive power generations are compared with their specified limits. If the calculated power violates its limits, the DG switches from droop-mode to PQ mode and the specified power is kept at the limit value.

In this work, the conventional droop equations expressed by (18) and (19) have been used in compliance with the IEEE standard 1547.4 for DG islanded systems. These characteristics are usually justified by assuming that the output impedance of the converter is mainly inductive due to the coupling inductor used at the converter output [8], the large inductor of the output filter or by the use of virtual inductive output impedance [30].

Load Flow Problem formulation

This section presents the load flow problem formulation in the rural islanded hybrid system. The relation between the branch voltages V_{ij} and branch currents I_{ij} between two nodes i and j can be expressed as follows:

$$|V_{ij}| = |Z_{ij}| |I_{ij}| \quad (20)$$

The branch currents can be obtained as a function of the branch voltages using

$$|I_{ij}| = |Y_{ij}| |V_{ij}| \quad (21)$$

For each bus i the injected power can be calculated as follows:

$$|S_{i,inj}| = |V_i| |I_{i,inj}|^{conj} \quad (22)$$

Where $|I_{i,inj}|^{conj}$ is the complex conjugate of the injected currents at node i . This injected current represents the sum of all the branch currents connected with bus i , therefore the injected current could be given by:

$$|I_{i,inj}| = \sum_{\substack{j=1 \\ j \neq i}}^{nbus} I_{ij} \quad (23)$$

Let $P_{i,inj}$ and $Q_{i,inj}$ denote the calculated active and reactive power injected to the hybrid system at each bus i . The bus current in terms of voltage and apparent power is:

$$I_{i,inj} = \frac{S_i^{conj}}{V_i^{conj}} = \frac{P_{i,inj} - jQ_{i,inj}}{V_i^{conj}} \quad (24)$$

$$\frac{P_{i,inj} - jQ_{i,inj}}{V_i^{conj}} = \sum_{j=1}^n Y_{ij} V_j \quad (25)$$

$$P_{i,inj} - jQ_{i,inj} = V_i^{conj} \sum_{j=1}^n Y_{ij} V_j = V_i \sum_{j=1}^n Y_{ij}^{conj} V_j^{conj} \quad (26)$$

By equating the real and imaginary terms of the above expression, two equations for each bus are derived in terms of four variables: P , Q , V , and the angle θ . The above equation for active and reactive power is solved using the Gauss-Seidel numerical method.

Application of Gauss-Seidel to Microgrid Load Flow Problems

The load flow problem in a standalone hybrid microgrid is characterized by the following salient features:

- There is no slack bus
- The system frequency is not constant
- The Y_{bus} matrix varies with the fluctuation of the frequency
- The line losses are not constant due to the variation in system voltages and frequency

To minimize divergence problems of the modified load flow algorithm, initial guesses of voltage and angle magnitudes are initially calculated using the conventional load flow algorithm. These initial guesses are then fed to the modified load flow algorithm.

Calculation of the voltage at all buses and the system losses: The voltage at all buses is calculated using the following expression:

$$V_{ii}^{k+1} = \frac{1}{Y_{ii}} \left[\frac{P_i - jQ_i}{(V_i^k)^*} - \sum_{n=1}^{i-1} (Y_{in} V_n^{k+1}) - \sum_{n=i+1}^N (Y_{in} V_n^k) \right] \quad (27)$$

Where V_i^{k+1} = Voltage for iteration $(k + 1)$ at bus i

Equation 31 gives both voltage magnitude and angle for the current iteration. It is worth noting that the algorithm requires the selection of a reference bus. When voltage is calculated for the selected reference bus, the resulting magnitude from equation 31 is kept while the angle is set back to zero. For droop-controlled buses, P_i and Q_i are estimated using equations 22 and 23, respectively. For all PQ or load buses, P_i and Q_i are constant and readily known through equations 25 and 26. For PV buses, active power and bus voltage are constant and preselected. The reactive power is evaluated using the following expression:

$$Q_i^{k+1} = -Im[(V_i^k)^* (\sum_{n=1}^{i-1} (Y_{in} V_n^{k+1}) - \sum_{n=i}^N (Y_{in} V_n^k))] \quad (28)$$

Once the reactive power generated at a PV bus is calculated, it must be verified to be within the Q limits of the unit. In case the calculated value lies beyond the maximum boundary, it must be set to Q_{max} . Secondly, when the voltage at the PV bus is calculated, the new bus angle is kept while the magnitude is setback to its pre-defined value. Droop equations are used to evaluate the active and reactive power output at VF buses.

Calculation of the new system frequency: Assuming that all DGs of the islanded microgrid are operating as droop based, it is assumed that the sum of all the active power generated by the DGs is equal to the total power circulating within the microgrid. Again, given that the frequency is the same in the entire microgrid, droop-controlled buses in the microgrid supply active power at the same angular frequency. Bidirectional converters are used to interface between DG units. Considering these observations, the following expression can be written:

$$P_{total} = P_{load} + P_{line_losses} = \sum_{i=1}^d P_{Gi} = \sum_{i=1}^d \frac{1}{m_{pi}} (\omega_0 - \omega) \quad (29)$$

From equation (29), the system frequency can be derived as follows:

$$\omega^{k+1} = \frac{\sum_{i=1}^d \frac{1}{m_{pi}} \omega_0 - (P_{load}^{k+1} + P_{line_loss}^{k+1})}{\sum_{i=1}^d \frac{1}{m_{pi}}} \quad (30)$$

Where d denotes droop-controlled generators

Calculation of the generated reactive power: The generated reactive power is evaluated and compared to the reactive power consumed by the loads. The total reactive power generated by droop-controlled generators can be derived from the expression relating the generated reactive power due to voltage mismatch, $V_{ref} - V_i$, and voltage droop coefficient, n_q . The reactive power generated at PV buses is calculated as shown in the previous section. To ensure that the reactive power demand of the system is met, the calculated new voltages must satisfy the following expression:

$$Q_{system} = \sum_{i=1}^g Q_{Gi} + Q_{PV} = \sum_{i=1}^g \frac{1}{n_{qi}} (V_0 - V_i) + Q_{PV} \quad (31)$$

Once the new frequency is evaluated, the new admittance matrix is re-calculated and the process is repeated to get the new bus voltages. The process is repeated until the error between the new ($k+1$) and the old (k) values of the voltages and the angular frequency is less than the pre-defined error margin. Again, the mismatch between the generated and consumed reactive power must be less than the error margin. Figure 4 depicts a flowchart which shows the steps involved in the modified load flow algorithm.

As shown in the flowchart of figure 4, the initial guesses of the unknown variables are calculated using the conventional load flow algorithm. This is to improve convergence. The initial values are then fed to the modified Gauss Seidel algorithm. In running the conventional load flow algorithm, all droop-controlled generators are assumed to be operated in PV -mode.

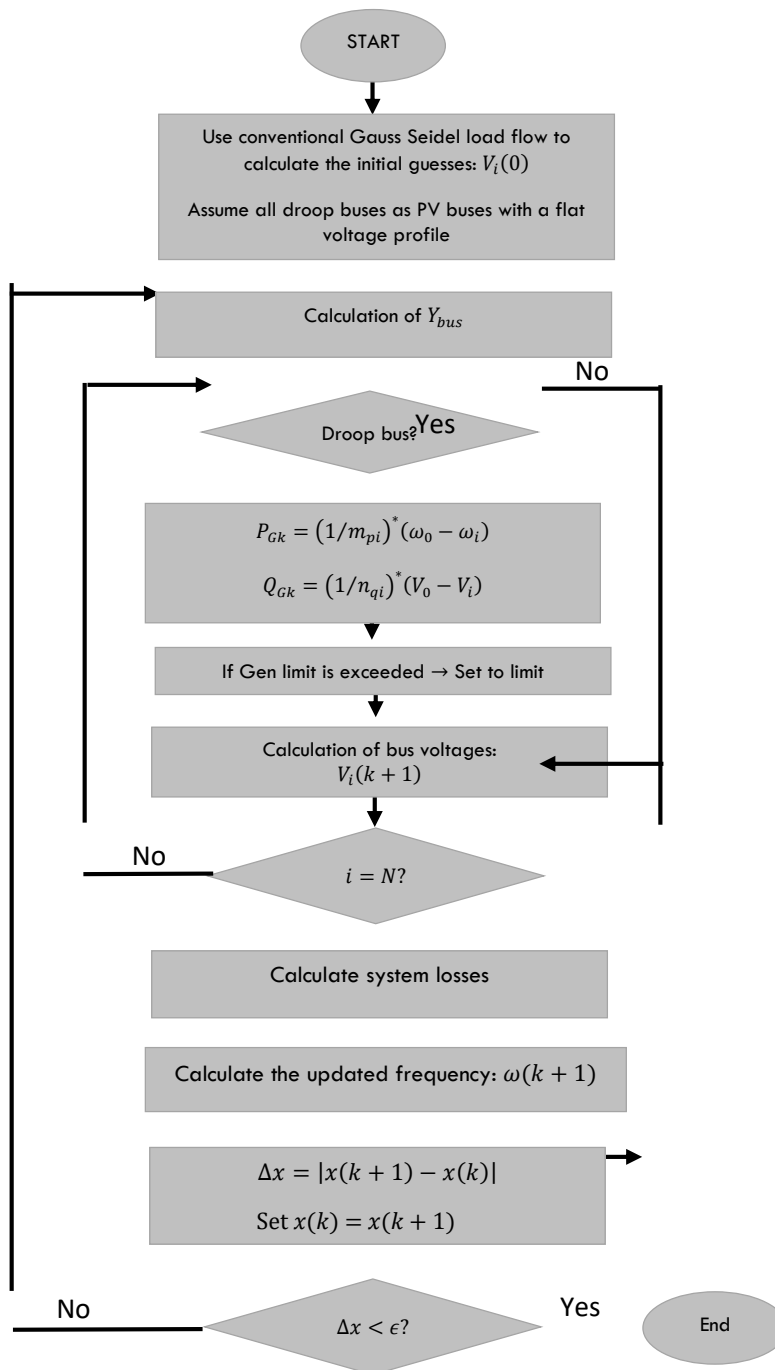


Figure 4: Flowchart of the Modified Gauss Seidel Load Flow Algorithm

4. RESULTS

Load Flow Algorithm Validation: To validate the applicability of the generalized load flow algorithm, the results of the proposed algorithm are compared with the steady-state results obtained from the conventional Gauss Seidel algorithm of the islanded hybrid system. The balanced 6-bus test system shown in Figure 5 has been used in the algorithm validation.

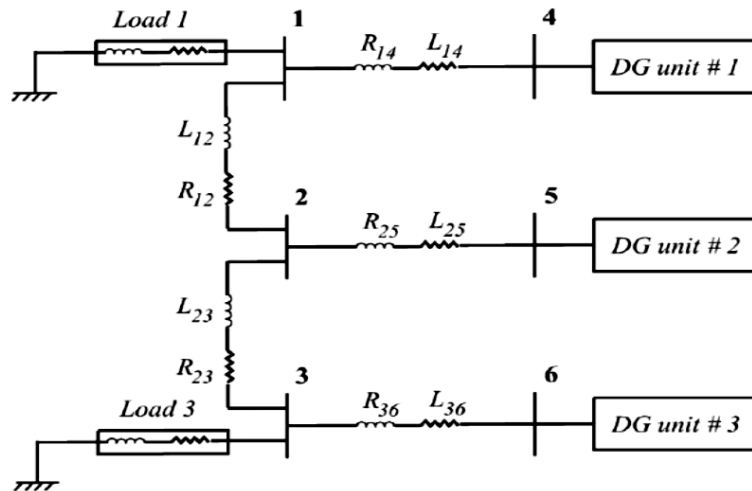


Figure 5: Single line diagram of the 6-bus microgrid test system

This system was chosen since it is adequately small, balanced and quite proportionate to small rural hybrid system. This system includes three identical droop-based DG units and represents an islanded hybrid system.

The data of the distribution test system are shown in tables 2, 4 and 4.

Table 2: p.u. Base Calculations

S_{base}, kVA	1
V_{base}, V (phase-phase)	220
Z_{base}, Ω	48.4
f, Hz	50

Table 3: Line Parameters of the Six-Bus Microgrid

Line Parameters (per phase)			
From bus	To bus	R_{line}	L_{line}
1	2	0.43	0.318
2	3	0.15	1.843
3	6	0.05	0.050
4	1	0.30	0.530
2	5	0.28	0.250

Table 4: Load parameters

System Load (per phase)		
Bus Number	Load Resistance (ohm)	Line Ind. (mH)
1	6.95	12.2
2	0	0
3	5.014	9.4
4	0	0
5	0	0
6	0	0

The results show the effectiveness of the proposed power flow algorithm in solving the droop controlled small islanded hybrid system networks. To show the limitation of the conventional load flow algorithms when it is applied to islanded microgrid with droop-controlled distributed generation units, a comparison between the results obtained by the proposed power flow algorithm and the results obtained from the conventional power flow algorithms are made. The conventional Gauss Seidel load flow algorithm assigns one DG unit as a slack bus and the other DG units as PV buses.

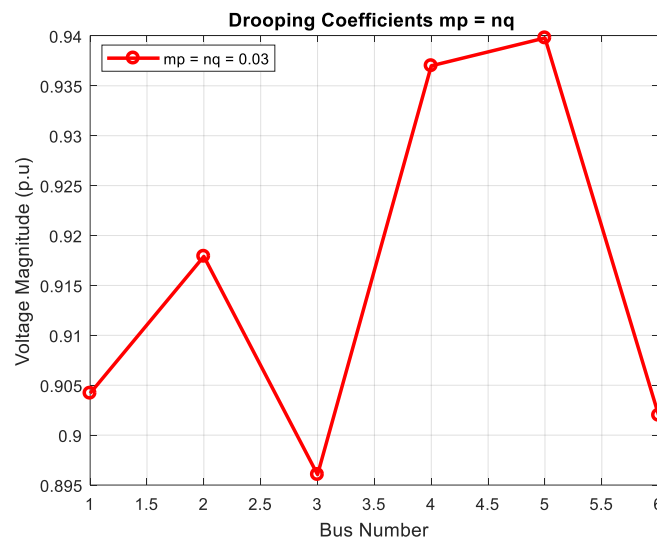


Figure 6: Bus voltages with rated droop settings

Figure 6 shows the plot of bus voltages. From the plot, it can be seen that the voltages at the generation buses are much higher than those of the load buses due to the line losses. It was also observed that the interconnecting bus (bus number 2) has a voltage higher than those of the load buses 1 and 3.

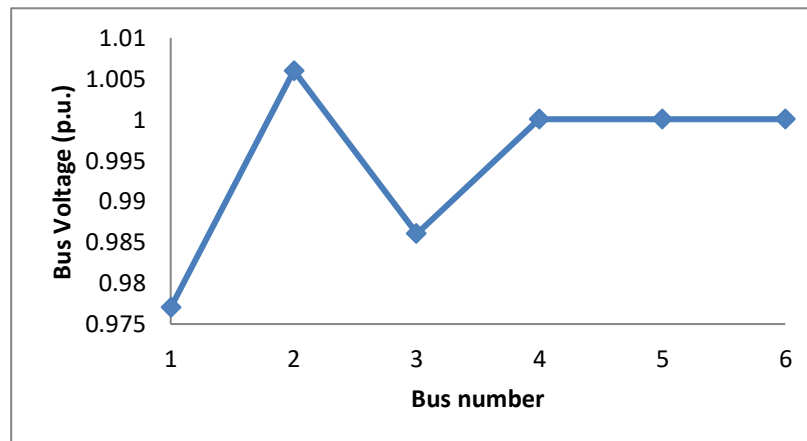


Figure 7: Bus Voltages with conventional GS

It is evident that the conventional gauss Seidel load flow algorithm does not capture the behaviour of droop controlled buses and therefore yields inaccurate results as shown in figure 7. The droop controlled buses (buses 4 and 5) were modelled as PV buses and bus 6 as slack bus. In the conventional GS load flow system, bus number 1 recorded the most significant drop and the interconnecting PQ bus (bus number 2) shows a voltage rise above rated value. This result does not reflect the actual operation of the microgrid because bus number 6 does not have the infinite characteristics of a slack bus.

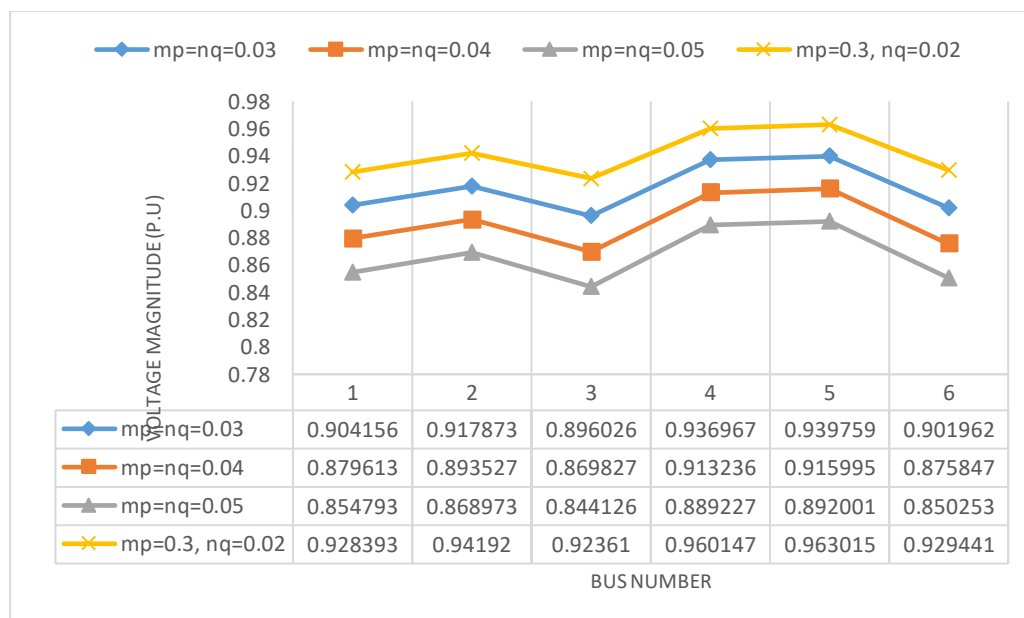


Figure 8: Voltages at buses with varied drooping coefficients

It is observed in figure 8 that variations in droop controls produce corresponding changes in frequency and voltage at the droop controlled buses. In order to capture the effects of changes in the frequency and voltage of the operating state, the speed droop control (active power static droop control mp) and the voltage droop control (reactive power static droop control nq) of all three droop controlled distributed generation units are varied. These changes depict the effect of using distributed generation resources with different drooping characteristics. The most appropriate drooping coefficients mp and nq for optimal voltage profile at the generator buses turned out from simulation to be 0.03 and 0.02 respectively and falls within the standards of NFPA in [31]

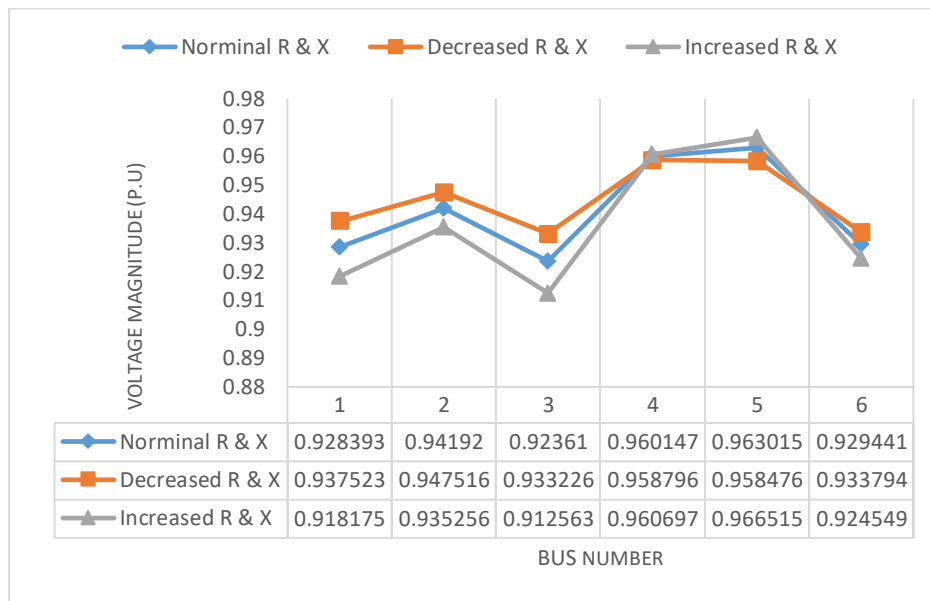


Figure 9: Effects of changes in line parameters on voltage drop at buses with mp set at 3% and np at 2%

The effects of line parameters on the voltage drop on the PQ buses for a given mp and nq set points is verified as show in figures 9, 10, 11 and 12. The results confirm that the voltage drop increases with increase in line parameters and drooping coefficients respectively.

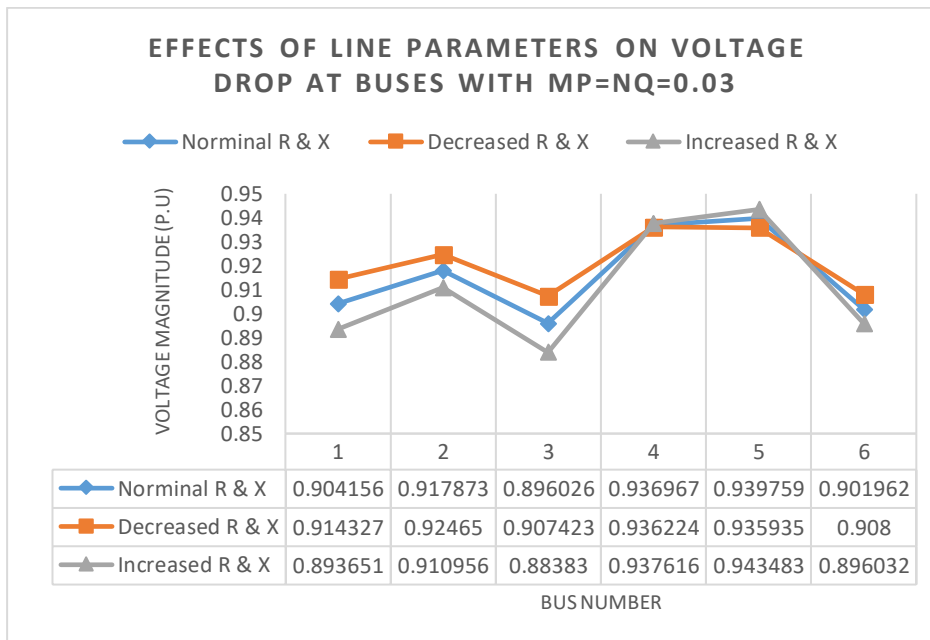


Figure 10: Effects of changes in line parameters on voltage drop at buses with mp = np = 3%

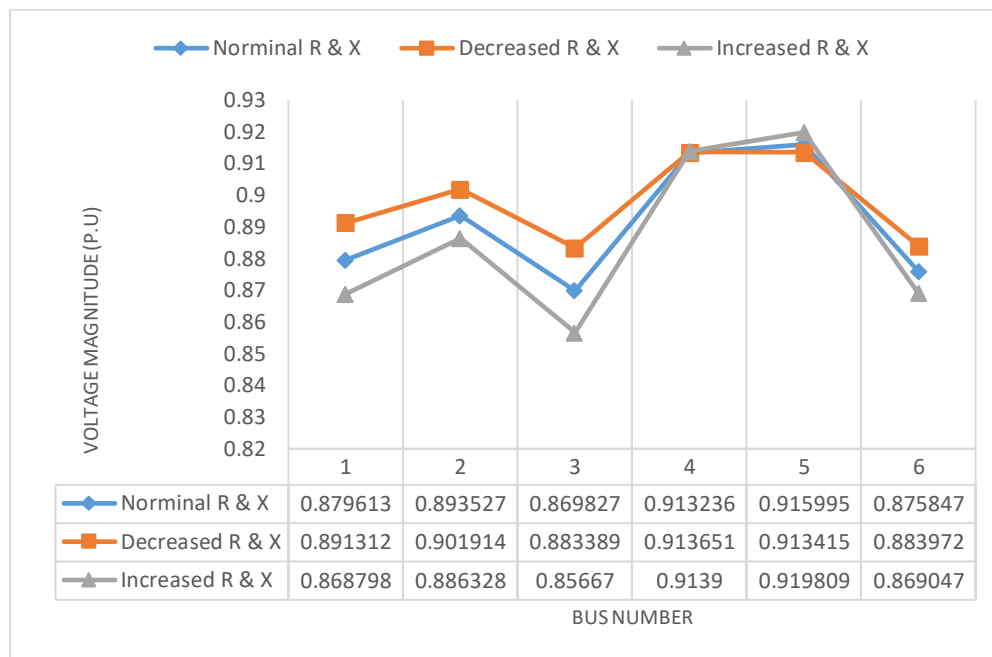


Figure 11: Effects of changes in line parameters on voltage drop at buses with $m_p = n_p$ at 4%

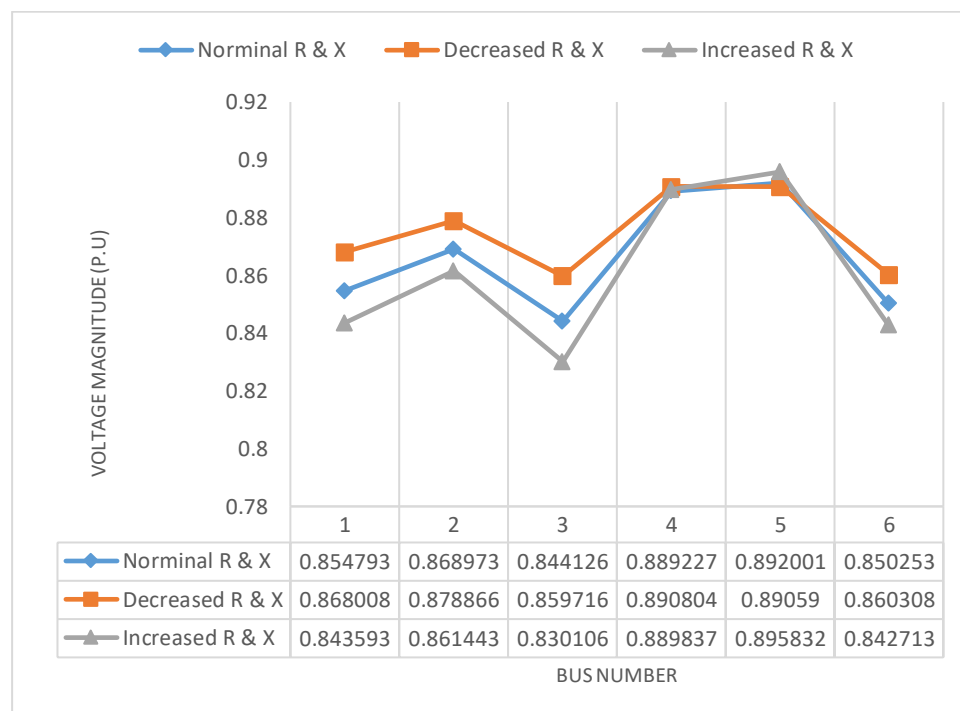


Figure 12: Effects of changes in line parameters on voltage drop at buses with $m_p = n_p = 5\%$

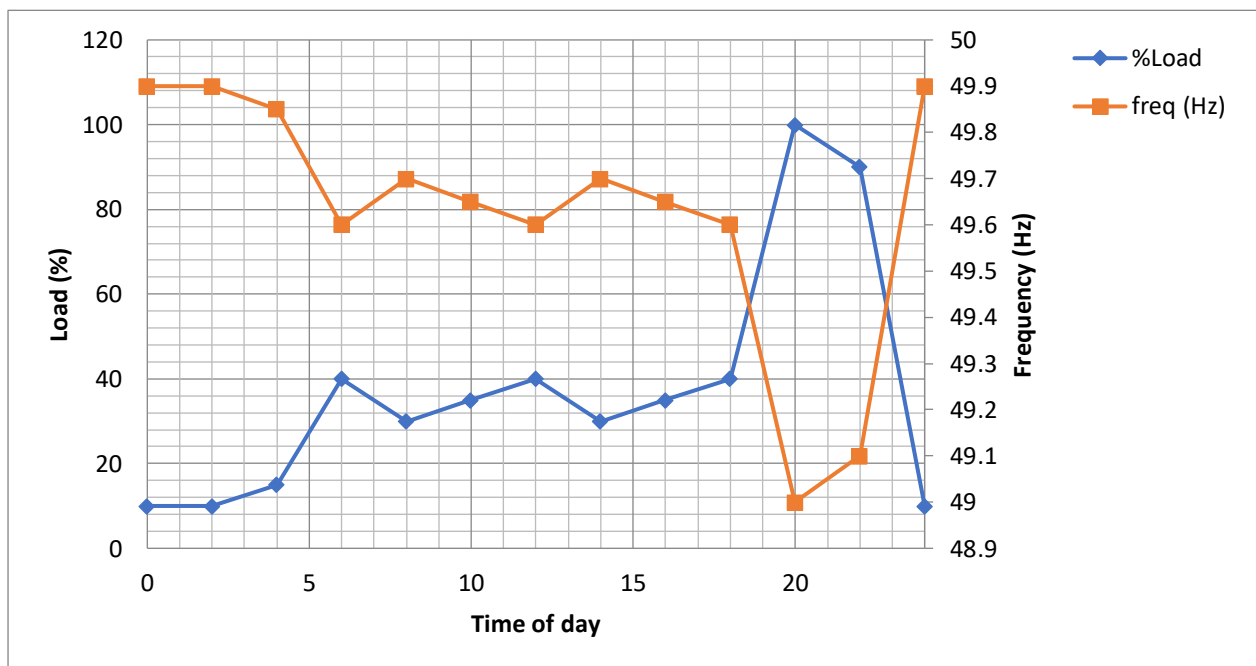


Figure 13: Load Profile and frequency variation

The system frequency was fairly constant between no-load and full load as shown in figure 13. As seen in figure 14, the frequency variation between no-load and full load is 0.9Hz. This value corresponds to that accepted by the NFPA standards [31].

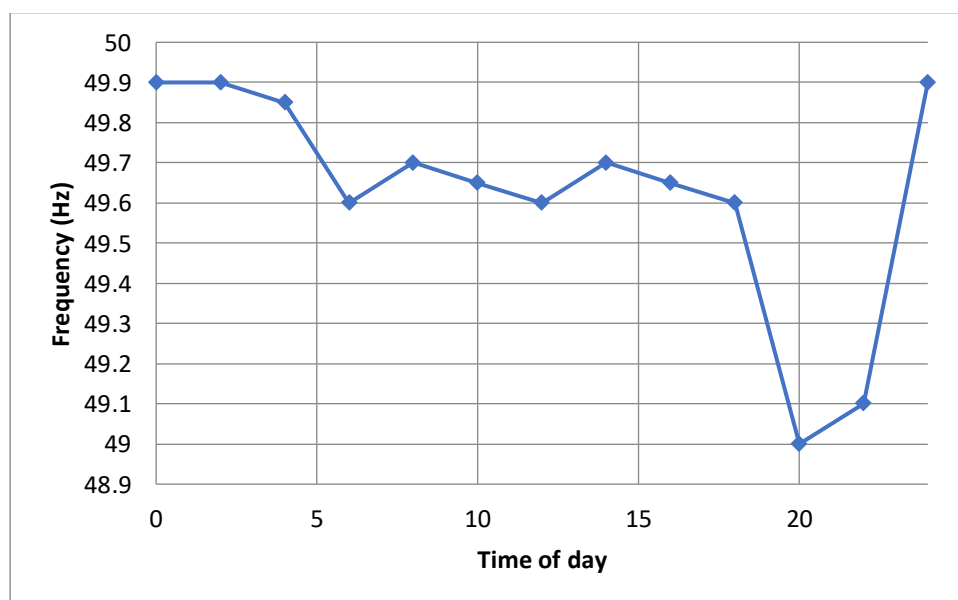


Figure 14: Frequency variation between no-load and full load

5. DISCUSSION

This study proposes a load flow algorithm to model the operation of balanced islanded hybrid systems for rural electrification. In order to mimic fully the off-grid operation, no slack bus was resorted to, given that the size of generators in a hybrid microgrid system are generally too small to assume the role of a slack generator. The generators of the studied system were modeled as droop-controlled buses, while the loads were modeled as PQ buses. The results obtained using the proposed generalized load flow algorithm showed a much better output that reflects the actual operation of a hybrid microgrid system. The proposed algorithm is a valuable tool to study the operation of islanded microgrids for small rural communities, especially during planning for extension. Again, the proposed algorithm allows for the efficient study of different aspects of the system, such as steady-state voltage profile, loading levels and frequency variation.

Hybrid renewable energy systems, though small-scaled, are endowed with high operational and constitutive sophistication. However, modern technology allows reliable and cost-competitive energy generation in remote areas, surpassing the convenience of traditional solutions using grid extension or diesel generation by economic and environmental considerations.

6. CONCLUSION

This work covers load flow on hybrid renewable energy system for rural electrification. The research exploits the implementation of a hybrid microgrid system. The main focus of this study is primarily related to the planning aspects of microgrids. When planning an electric network, one of the major operating states considered is the steady state operation. The steady-state aspect is concerned with voltage stability, loading levels of the feeders and frequency limits. These aspects are investigated through steady-state analysis which relies on load flow algorithms.

Whenever a hybrid microgrid is envisaged, it is essential to study it under islanded operation given that this is the most constraining condition. The hybrid microgrid has to regulate its own voltage and frequency while meeting load demand. In order to achieve this goal, distributed generation units in hybrid microgrids are usually operated in droop-control mode. Under this mode of operation, the output active power of the distributed generation units is not set to a pre-specified value but rather adjusted with respect to changes in system frequency. Similarly, the reactive power output of these generators is calibrated against the voltage level at the connecting bus. These droop-control complexities are not considered in conventional load flow algorithms hence, these algorithms lead to very inaccurate and misleading load flow results. The load flow algorithm proposed in this paper allows simulating all aspects of droop-controlled islanded microgrids in steady-state operation.

REFERENCES

- [1] J. B. Gupta, A Course in Electric Power, New Delhi: S.K. Kataria & Sons, 2013.
- [2] Cameroon Fact Sheet, State of Energy sector (supply/demand), Cameroon Fact Sheet, December, 2012.
- [3] I. E. Agency, "World Energy Outlook 2024," International Energy Agency, 2024.
- [4] A. Zambroni and M. Castilla, Microgrids Design and Implementation, Cham: Springer Nature Switzerland AG, 2019.
- [5] D. Das, Electrical Power Systems, New Delhi: New Age International Ltd, 2006.
- [6] P. Y. Lakshmi, "Power Flow Analysis of Integrated Wind and Solar Power Generation and Distribution System," International Journal of Engineering Research & Technology (IJERT), vol. V, no. 06, June-2016, pp. 214-216, 2016.
- [7] A. NUR and A. KAYGUSUZ, "POWER FLOW STUDY FOR A MICROGRID BY USING MATLAB AND POWERWORLD SIMULATOR," International Journal of Energy and Smart Grid, vol. 1, 2016.
- [8] N. Pogaku, M. Prodanovic and T. Green, "Modeling, analysis and testing of autonomous operation of an inverter-based microgrid," IEEE Trans. Power Electron, vol. 22, no. 2, pp. 613-625, 2007.
- [9] F. Mumtaz, M. H. Syed, M. Al Hosani and H. H. Zeineldin, "A novel approach to solve power flow for islanded microgrids using modified Newton Raphson with droop control of DG," IEEE Transactions on Sustainable Energy, vol. 7, no. 2, p. 493–503, 2016.
- [10] E. R. Sanseverino, M. L. Di Silvestre, R. Badalamenti, N. Q. Nguyen, J. M. Guerrero and L. Meng, "Optimal power flow in islanded microgrids using a simple distributed algorithm," Energies, vol. 8, no. 10, p. 11493–11514, 2015.
- [11] V. Kaur and S. Grover, "INCLUDING SLACK BUS IN NEWTON RAPHSON METHOD FOR LOAD FLOW SOLUTION: A REVIEW," Journal of Emerging Technologies and Innovative Research (JETIR) , vol. 6, no. 5 May 2019, pp. 142-146, 2019.
- [12] A. Felix, M. Farret and S. Goodoy, Integration of Alternative Sources of Energy, New Jersey: John Wiley and Sons Inc., 2006.
- [13] S. Yeleli and Y. Fu, "Impacts of energy storage on future power systems," in IEEE North American Power Symposium, 2010.
- [14] A. C. Z. De Souza, M. Santos, M. M. J. Castilla, L. G. de Vicuña and D. Marujo, Microgrids Design and Implementation, Cham: Springer Nature Switzerland AG, 2019.
- [15] J. Jenson and B. Sorenson, Fundamentals of Energy Storage, New York: John Wiley and Sons Inc., 1984.
- [16] M. Abedini, "A New Algorithm for Load Flow Analysis in Autonomous Networks," International Journal of Smart Electrical Engineering, vol. 5, pp. 176-182, 2016.
- [17] N. Lidula and A. Rajapakse, "Microgrids research: A review of experimental microgrids and test systems," Elsevier Ltd, Renewable and Sustainable Energy Reviews, vol. 15, pp. 186-202, 2011.
- [18] J. Rocabert, A. Luna, F. Blaabjerg and P. Rodríguez, "Control of power converters in AC microgrids," IEEE Transactions on Power Electronics, vol. 27, no. 11, pp. 4734-4749, 2012.
- [19] S. J. Chapman, Electric Machinery Fundamentals, New York: McGraw Hill, 1999.
- [20] Mehmet Şefik Üney, Halil Çimen, Nurettin Çetinkaya and Mehmet Latif Levent, "Optimal Power Flow and Load Flow Analysis with Considering Different DG Integration Rates," Asian Journal of Applied Science and Technology (AJAST), vol. 1, no. 9, pp. 542-549, 2017.

- [21] P. Harish Kumar and Mageshvaran R., "Load Flow Analysis and Optimal allocation of DG for Indian Utility 62 Bus Power system," International Journal on Emerging Technologies , vol. 11, no. 2, pp. 874-886, 2020.
- [22] S. Anbuchandran, R.Rengaraj, D. Silas Stephen, M. Arumuga Babu, "Power flow study of a power system with distributed generators," NeuroQuantology , vol. 20 , no. 10, pp. 9001-9013, 2022.
- [23] Aya Al Shaltouni and Abdulla Ismail, "Smart Load Flow Analysis using Conventional method and modern method," International Journal of Automation and Digital Transformation, vol. 1, no. 1, pp. 60 - 86, 2023.
- [24] T. F. o. L. R. f. D. P. IEEE, "Bibliography on load models for power flow and dynamic performance simulation," IEEE Trans. Power Syst., vol. 10, no. 1, pp. 523-538, February 1995.
- [25] P. Kundur, Power System Loads in Power System Stability and Control, New York: McGraw-Hill, 1994.
- [26] F. Blaabjerg, Z. Chen and S. B. Kjaer, "Power electronics as efficient interface in dispersed power generation systems," IEEE Transactions on Power Electronics, vol. 19, no. 5, pp. 1184-1194, 2004.
- [27] P. N, P. M and G. T, "Modeling, analysis and testing of autonomous operation of an inverter-based microgrid," IEEE Trans. Power Electron., vol. 22, no. 2, pp. 613-625, March 2007.
- [28] M. Prodanovic, T. Green and H. Mansir, "A survey of control methods for parallel three-phase inverters connection," Proc. Inst. Elect. Eng., pp. 472-477, 2000.
- [29] T. Green and M. Prodanovic, "Control of inverter-based micro-grids," Elect. Power Syst. Res., vol. 77, no. 9, pp. 1204-1213, July 2007.
- [30] M. Guerrero, L. De-Vicuna, J. Matas and M. M. J. Castilla, "Output impedance design of parallel connected UPS inverters with wireless load-sharing control," IEEE Trans. Ind. Electron., vol. 52, no. 4, pp. 1126-1135, August 2005.
- [31] Abadgostar Tasisat Iraninan Co.,LTD, Electrical Standard for Industrial Machinery, Orlando: National Fire Protection Association, 2007.